This is the accepted manuscript made available via CHORUS. The article has been published as:

Evolution from B_{2g} Nematics to B_{1g} Nematics in Heavily Hole-Doped Iron-Based Superconductors

Vladislav Borisov, Rafael M. Fernandes, and Roser Valentí

Phys. Rev. Lett. **123**, 146402 — Published 30 September 2019

DOI: 10.1103/PhysRevLett.123.146402

Evolution from B_{2g} nematics to B_{1g} nematics in heavily hole-doped iron-based superconductors

Vladislav Borisov,[1] Rafael M. Fernandes,[2] and Roser Valentí[1]

[1] *Institute of Theoretical Physics, Goethe University Frankfurt am Main, D-60438 Frankfurt am Main, Germany**
[2] *School of Physics and Astronomy, University of Minnesota, Minneapolis, Minnesota 55455, USA*

(Dated: September 13, 2019)

Recent experiments reported an unusual nematic behavior of heavily hole-doped pnictides $A\mathrm{Fe_2As_2}$, with alkali A = Rb, Cs. In contrast to the B_{2g} nematic order of the parent $Ae\mathrm{Fe_2As_2}$ compounds (with alkaline earth Ae = Sr, Ba), characterized by unequal nearest-neighbor Fe-Fe bonds, in the hole-doped systems nematic order is observed in the B_{1g} channel, characterized by unequal next-nearest-neighbor Fe-Fe (diagonal Fe-As-Fe) bonds. In this work, using density functional theory, we attribute this behavior to the evolution of the magnetic ground state along the series $Ae_{1-x}A_x\mathrm{Fe_2As_2}$, from single stripes for small x to double stripes for large x. Our simulations using the reduced Stoner theory show that fluctuations of Fe moments are essential for the stability of the double-stripe configuration. We propose that the change in the nature of the magnetic ground state is responsible for the change in the symmetry of the vestigial nematic order that it supports.

PACS numbers:

Introduction. Unconventional superconductivity in iron-based superconductors is believed to be mediated by spin fluctuations and, therefore, closely related to the nature of the magnetic interactions[1,2]. The most common type of magnetic order – single-stripe phase – is observed is many parent compounds, such as $Ae\mathrm{Fe_2As_2}$ (Ae = Ca, Sr, Ba)[3–5]. Stripe magnetic order is characterized by an ordering vector $(\pi, 0)$ or $(0, \pi)$ in the Fe-only square lattice. As such, it breaks the tetragonal symmetry of the lattice by making the nearest-neighbor Fe-Fe bonds inequivalent. External pressure or chemical substitution suppress this magnetic order and induce superconductivity (SC), suggesting a close link between the two phases. Besides possibly providing the glue that binds Cooper pairs together, magnetic fluctuations are also believed to be responsible for the nematic phase of the $Ae\mathrm{Fe_2As_2}$ compounds[6]. This is corroborated by the experimental observation that the magnetic and nematic transition lines follow each other closely, and that the elastic and magnetic fluctuations obey a scaling relationship[7,8]. One of the proposed mechanisms by which nematicity arises before the onset of single-stripe magnetic order is that magnetic fluctuations form a composite order parameter that condenses above the magnetic transition. In this scenario, nematic order is a vestigial phase of the magnetically ordered phase, breaking a subset of the symmetries broken by the latter (i.e. tetragonal symmetry) while preserving other symmetries (i.e. time-reversal symmetry)[9–12].

Very recently, a different type of nematic order was found in the stoichiometric $\mathrm{RbFe_2As_2}$ and $\mathrm{CsFe_2As_2}$ compounds[13–15]. Because these materials have an n_d = 5.5 filling of the Fe $3d$ orbitals, in contrast to the $n_d = 6$ filling of the $Ae\mathrm{Fe_2As_2}$ compounds, they are heavily hole-doped versions of the latter. The nematic order displayed by $\mathrm{RbFe_2As_2}$ lowers the tetragonal symmetry by breaking the equivalence between the next-nearest-neighbor Fe-Fe bonds, which correspond to the diagonals of the Fe-only square lattice. In group-theory language, this corresponds to a B_{1g} nematic state, whereas the nematic state of $Ae\mathrm{Fe_2As_2}$ is in the B_{2g} channel (see insets in Fig. 1 and 4). Here, B_{1g} and B_{2g} refer to the irreducible representations of the tetragonal point group associated with the actual crystallographic unit cell, which contains two Fe atoms and is rotated 45° with respect to the Fe-only square unit cell. An important question that remains unaddressed is the origin of this B_{1g} nematic state. A recent theoretical study[16] proposes that this new type of nematicity is driven by incommensurate spin fluctuations on d_{xy} orbitals, and is related to the Lifshitz transition as the system goes from $n_d = 6$ to $n_d = 5.5$ filling. On the other hand, structural differences between these systems can, in principle, produce significant changes in the magnetic interactions too, similarly to the well-known case of $\mathrm{FeSe}_x\mathrm{Te}_{1-x}$.[17] Moreover, electronic correlations are believed to be much stronger in $\mathrm{RbFe_2As_2}$ and $\mathrm{CsFe_2As_2}$ as compared to $Ae\mathrm{Fe_2As_2}$, as manifested by the larger Sommerfeld coefficients of the former[18] and suggested by theoretical studies based on the LDA+DMFT method.[19–22]

In this paper, we address the change of nematic order from B_{2g} to B_{1g} as a function of hole-doping in a specific 122 family $\mathrm{Sr}_{1-x}\mathrm{Rb}_x\mathrm{Fe_2As_2}$. In particular, we use first-principles density functional theory (DFT) calculations to analyze the competition between different magnetic orders as the iron $3d$ orbital filling evolves from 6 to 5.5 for increasing x. These DFT calculations include the effects of i) hole doping, ii) structural changes and, iii) Fe moment reduction by spin fluctuations within the recently proposed reduced Stoner theory.[23,24] We find that the favored magnetic ground state changes from single-stripe to double-stripe, which is characterized by an ordering vector of $(\pi/2, \pi/2)$ in the Fe-only square Brillouin zone. The main results are shown in the phase diagram of Fig. 1 which spans different systems between $\mathrm{SrFe_2As_2}$ and $\mathrm{RbFe_2As_2}$ and summarizes the effects of

doping and lattice strain on the competition between the single- and double-stripe orders. The stabilization of the double-stripe order in $RbFe_2As_2$, as compared to the single-stripe order in $SrFe_2As_2$, arises primarily from the changes in the electron count, rather than the changes in the lattice structure, and seems to be unrelated to Fermi surface nesting. Since the B_{2g} nematic order is a vestigial phase of the single-stripe phase, whereas the B_{1g} nematic order is a vestigial phase of the double-stripe phase, our results provide a unified picture in which the change in the nematic state as function of hole-doping reflects a change in the dominant magnetic interactions.

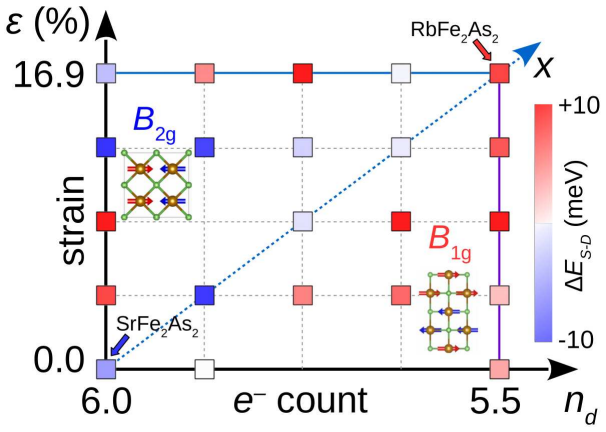

FIG. 1: Schematic magnetic phase diagram of $Sr_{1-x}Rb_xFe_2As_2$ as function of strain (in %) along the c-axis and Fe $3d$ electron count. Both parameters are tuned simultaneously as function of x, interpolating between the two end compounds, $SrFe_2As_2$ ($\varepsilon = 0\%$ and $n_d = 6.0$) and $RbFe_2As_2$ ($\varepsilon = 16.9\%$ and $n_d = 5.5$). The two types of magnetic ground states are shown by color (red – double stripe, blue – single stripe), and the color intensity reflects the energy difference $\Delta E_{\mathrm{S-D}} = E_{\mathrm{single}} - E_{\mathrm{double}}$ between these two magnetic orders (in meV/Fe). The phase diagram only shows the data points where the calculations for both magnetic states converged.

First-principle results: magnetic order. We focus on the series $Sr_{1-x}Rb_xFe_2As_2$, since, among the three AFe_2As_2 stoichiometric compounds, A = Rb is the one that displays the strongest evidence for B_{1g} nematic order,[14,15] as compared to A = Cs and A = K. The choice of Sr is to minimize steric effects related to the different sizes of the cations. Also, this study should motivate the corresponding experiments verifying the results in Fig. 1, since so far only the end compounds were investigated in the context of nematicity. To perform our DFT calculations, we used for the stoichiometric compounds $RbFe_2As_2$ and $SrFe_2As_2$ the experimental room-temperature structures, both belonging to the $I4/mmm$ space group (Rb: $a = 3.87198$ Å, $c = 14.46$ Å, $z_{\mathrm{As}} = -0.1525$; Sr: $a = 3.9243$ Å, $c = 12.3644$ Å, $z_{\mathrm{As}} = -0.14$).[25,26] The structural parameters of the series $Sr_{1-x}Rb_xFe_2As_2$ were obtained by linear interpolation of the lattice parameters and all bond lengths following the equations:[46]

$$\begin{aligned} \hat{a}_{\mathrm{int}} &= \hat{a}_1 + x \cdot (\hat{a}_2 - \hat{a}_1) \\ \mathbf{r}_{\mathrm{int}} &= \mathbf{r}_1 + x \cdot (\hat{a}_{\mathrm{int}})^{-1} \hat{a}_2 (\mathbf{r}_2 - \mathbf{r}_1) \end{aligned} \tag{1}$$

Here, $\hat{a}$ is the matrix of the lattice vectors and $\mathbf{r}$ is a vector of fractional coordinates of a given atom in the supercell. The indices 1, 2 and "int" refer to $SrFe_2As_2$, $RbFe_2As_2$ and $Sr_{1-x}Rb_xFe_2As_2$, respectively. For $Sr_{1-x}Rb_xFe_2As_2$, the spacer cation is replaced by an artificial atomic species with a fractional nuclear charge of $Z = 38 - x$, which simulates a random mixture of Sr and Rb using the virtual crystal approximation.

The competition between the non-magnetic state and three different types of magnetic states (single-stripe, Néel, and double-stripe) in this compound series was studied using the FLAPW method as available in the ELK code.[30] Fully relativistic magnetic energies were calculated using the PBE parameterization[31] of the GGA density functional. The number of empty states was set to 24 per atom and spin, whereas the smearing was set to 0.002 Ha ≈ 50 meV and the k-mesh dimensions to $(10 \times 10 \times 10)$. The aforementioned magnetic configurations – single-stripe, Néel, and double-stripe – are the usual competitors in Fe-based superconductors and have different spatial periodicities corresponding to the ordering vectors (in the coordinate system of the Fe-only square lattice) $\mathbf{Q}_1 = (\pi, 0)$, $\mathbf{Q}_2 = (\pi, \pi)$ and $\mathbf{Q}_3 = (\pi/2, \pi/2)$, respectively. In this work, these states are simulated using the minimal 8-Fe supercells of different shapes (see insets in Figs. 1 and 2). Each supercell includes a second Fe layer where all spins point in the opposite directions, which is commonly observed in iron pnictides.[32–34] Although the energy competition between different types of the magnetic alignment along the c-direction may not be accurately captured in our DFT-based approach with reduced Fe moments, we have verified that the nematic behavior is not affected qualitatively by a particular choice of the c-axis ordering.

One important ingredient of the physics in the iron-based superconductors that is often not captured by standard DFT approaches is the role of spin fluctuations. They are essential for instance to explain the reduced magnetic moment of the Fe atoms, which is usually overstimated in DFT.[24] Here, spin fluctuations are modeled using the reduced Stoner theory[23] with a single adjustable parameter s that scales down the spin splitting of the self-consistent potential $V(\mathbf{r})$ which enters then the DFT equations as:

$$V'_{\uparrow}(\mathbf{r}) - V'_{\downarrow}(\mathbf{r}) = s(V_{\uparrow}(\mathbf{r}) - V_{\downarrow}(\mathbf{r})) \tag{2}$$

The role of s is essentially to enhance the amplitude of the magnetic fluctuations, which in turn results in a suppression of the Fe magnetic moments. For the family of doped $CaFe_2As_2$ compounds, it has been found that values around $s = 0.85$ provide a consistent and precise description of the Fe magnetic moments as a function of temperature and doping.[24] For this reason, hereafter we

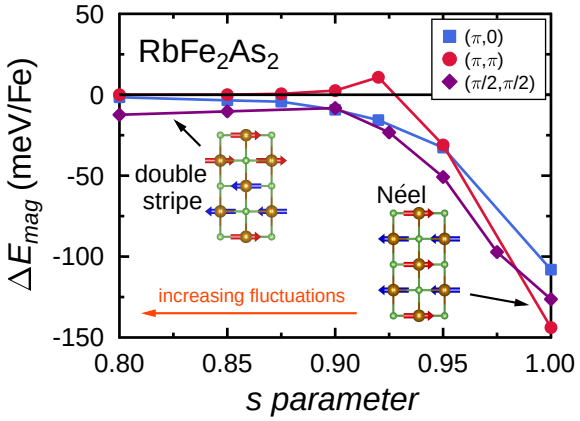

FIG. 2: Total energies of the magnetic orders in $RbFe_2As_2$ with different ordering vectors: $(\pi, 0)$ (single stripe), (π, π) (Néel order), and $(\pi/2, \pi/2)$ (double stripe) relative to the non-magnetic state ($\Delta E_{\rm mag} = E_{\rm mag} - E_{\rm non\text{-}mag}$). The insets show the Fe spin configuration for the double-stripe and Néel orders. The energies are calculated for the experimental structure as functions of the s parameter of the reduced Stoner theory (RST). The GGA limit corresponds to $s = 1$, while $s < 1$ leads to reduced Fe moments.

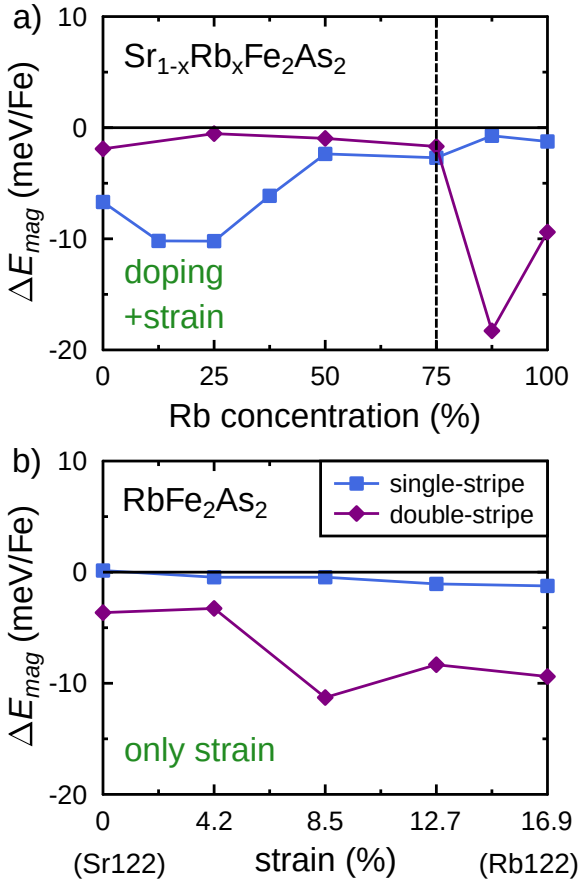

FIG. 3: Evolution of magnetic energies relative to the non-magnetic state ($\Delta E_{\rm mag} = E_{\rm mag} - E_{\rm non\text{-}mag}$) for the single- (squares) and double-stripe (diamonds) orders in (a) the series $Sr_{1-x}Rb_xFe_2As_2$ and (b) $RbFe_2As_2$ under c-axis strain. In both cases, the structure is tuned according to Eq. (1). The parameter in the reduced Stoner model, Eq. (2), is fixed to $s = 0.85$, which brings the Fe moments close to the typically measured values below $0.7\,\mu_{\rm B}$.

set $s = 0.85$ in our calculations. It turns out that correctly capturing these enhanced spin fluctuations is crucial for the magnetic ground state, as indicated by the calculated magnetic energies for $RbFe_2As_2$ versus the s parameter (Fig. 2). For the values around $s = 0.85$, the double-stripe is the dominating magnetic configuration showing the correct order of magnitude of Fe moments $\sim 0.5\,\mu_{\rm B}$.[47] At the same time, the single-stripe order strongly competes with this double-stripe ground state, while the Néel order is fully suppressed. In contrast, $s = 1$ leads to overestimated Fe moments of the order of $2\mu_B$, commonly observed in previous DFT simulations of iron-based systems,[35] and the nature of the magnetic ground state of $RbFe_2As_2$ changes dramatically. Nevertheless, our results are robust for a reasonably wide range of values of s corresponding to small Fe moments usually measured in experiments.[34]

In the next step, we study the evolution of magnetic energies for $Sr_{1-x}Rb_xFe_2As_2$ with simultaneous hole-doping x and lattice deformation (Fig. 3a). As shown in Fig. 3a, the single-stripe order of the parent $SrFe_2As_2$ compound is the ground state up to a Rb concentration of about 75%, where the magnetic ground state switches to the double-stripe. At this point, the Fe occupation is $n_d = 5.625$, compared to $n_d = 6$ for pure $SrFe_2As_2$. The exact value of the critical Rb concentration driving a double-stripe configuration might depend on subtle structural changes induced by doping, which are not captured in our approach based on linearly interpolated structures.

In these simulations the effects of the electron count and the lattice parameters are both present. In order to disentangle their role in driving the double-stripe order in $RbFe_2As_2$, we compute the magnetic energies when the structural parameters are tuned between those of $SrFe_2As_2$ and $RbFe_2As_2$, according to Eq. (1), and the Fe electron count is fixed at $n_d = 5.5$ (hole-doped regime). The main change in the lattice parameters is a stretch of the c-axis corresponding to a strain of ~17%. Importantly, such a stretch also affects various bond lengths. As shown in Fig. 3b, for all strain values investigated, the energy of the single-stripe magnetic state is always higher than that of the double-stripe state. On the other hand, variation of the electron count in the fixed $RbFe_2As_2$ structure changes the dominant magnetic configuration. Even more complex behavior is observed when both parameters – electron count n_d and strain ε – are varied simultaneously (Fig. 1). There is, however, a clear trend that large hole doping favors the double-stripe order. Interestingly, the phase diagram in Fig. 1 suggests that, for a fixed electron count between $n_d = 5.5$ and $n_d = 6.0$, the nature of the underlying magnetic order can be dramati-

cally changed by the lattice strain. These results indicate that both the bond lengths and the electron filling of the Fe $3d$ orbitals play a significant role for the character of magnetic interactions in the considered iron-based systems.

Vestigial nematic orders. So far our DFT simulations show a change in the magnetic ground state of $Sr_{1-x}Rb_xFe_2As_2$ from single-stripe, for small and moderate x, to double-stripe for large x. As we now argue, this evolution of the magnetic phase naturally accounts for the change in the nematic state from B_{2g} (small and moderate x) to B_{1g} (large x) observed experimentally. The key point is that both the single-stripe and the double-stripe states support symmetry-breaking composite order parameters that can condense even in the paramagnetic phase, forming so-called vestigial phases.[36]

The case of the single-stripe phase has been widely studied[9–12]. The Ising-like composite spin order parameter $\Phi_{B_{2g}} = \langle \mathbf{S}_{\mathbf{R}_i} \cdot \mathbf{S}_{\mathbf{R}_i+\mathbf{x}} \rangle - \langle \mathbf{S}_{\mathbf{R}_i} \cdot \mathbf{S}_{\mathbf{R}_i+\mathbf{y}} \rangle$ is clearly non-zero and uniform in the single-stripe phase, since spins are parallel to each other along one axis and anti-parallel to each other along the other axis (see Fig. 4a). As shown by a variety of different theoretical methods[9–12], $\Phi_{B_{2g}}$ can remain non-zero even when there is no long-range magnetic order, $\langle \mathbf{S}_{\mathbf{R}_i} \rangle = 0$, because $\Phi_{B_{2g}}$ is a two-spin correlation function. Now, since $\Phi_{B_{2g}}$ breaks the equivalence between the x and y axis, its onset breaks tetragonal symmetry, while preserving translational symmetry. The state with $\Phi_{B_{2g}} \neq 0$ but $\langle \mathbf{S}_{\mathbf{R}_i} \rangle = 0$ is a B_{2g} nematic state. It is called a vestigial phase of the magnetically ordered state because it breaks a subset of the symmetries broken by the latter, as explained in the Introduction.

Analogously, inside the double-stripe magnetic phase, the Ising-like composite order parameter $\Phi_{B_{1g}} = \langle \mathbf{S}_{\mathbf{R}_i} \cdot \mathbf{S}_{\mathbf{R}_i+\mathbf{x}+\mathbf{y}} \rangle - \langle \mathbf{S}_{\mathbf{R}_i} \cdot \mathbf{S}_{\mathbf{R}_i-\mathbf{x}+\mathbf{y}} \rangle$ is non-zero and uniform[37], since spins are parallel along one diagonal and anti-parallel along the other diagonal (see Fig. 4b). In this case, a vestigial B_{1g} nematic phase, in which diagonals are not equivalent, can appear even in the absence of long-range magnetic order[38,39]. Thus, the change in the magnetic ground state from single-stripe to double-stripe should be accompanied by a change in the vestigial nematic order from B_{2g} to B_{1g}.

An interesting question that remains to be addressed is why $RbFe_2As_2$ shows nematic order but no apparent sign of long-range magnetic order, whereas $SrFe_2As_2$ displays both magnetic and nematic orders.[40] The situation seems to be similar to the case of the Ti-based oxypnictides[38], where a B_{1g} vestigial nematic phase driven by double-stripe magnetic fluctuations has been proposed, but long-range magnetic order has not been observed. First, it is important to recall that the nematic transition, which must always happen above or simultaneously to the magnetic transition, is observed at lower temperatures in $RbFe_2As_2$ ($T_{\rm nem} \sim 40\,{\rm K}$)[14] as compared to $SrFe_2As_2$ ($T_{\rm nem} \sim 200\,{\rm K}$).[40] Second, the existence of competing magnetic states that support the same vestigial nematicity leads to frustration and suppression of long-range magnetic order, but enhancement of the vestigial order. In a previous work on FeSe,[41] the magnetic states with the ordering vectors $q = (\pi/n, 0)$ ($n = 2, 3, 4 \ldots$) were found to have very close energies which prevents long-range magnetic order but still supports B_{2g} nematicity. In the case of $RbFe_2As_2$, the magnetic configurations compatible with B_{1g} nematicity are those with the ordering vectors $q = (\pi/n, \pi/n)$. Our DFT calculations show that already the state with $n = 3$ (triple stripe) has almost the same energy as the double stripe. This can explain the absence of long-range magnetism in $RbFe_2As_2$, despite the emergence of nematic order.

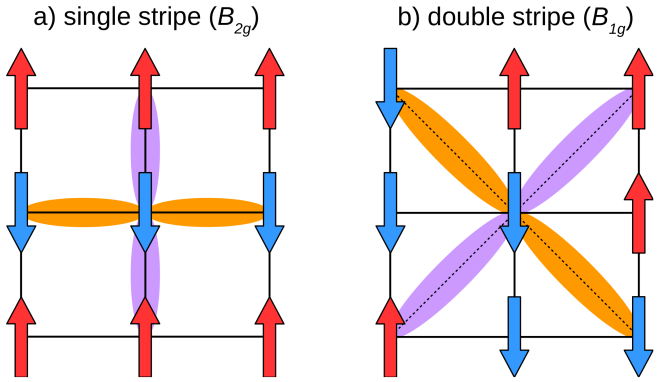

FIG. 4: Schematic representations of (a) the vestigial B_{2g} nematic phase associated with the single-stripe magnetic phase and (b) the vestigial B_{1g} nematic phase supported by the double-stripe magnetic phase. The lobes illustrate the spin-spin correlation functions entering the Ising-like composite order parameters $\Phi_{B_{2g}} = \langle \mathbf{S}_{\mathbf{R}_i} \cdot \mathbf{S}_{\mathbf{R}_i+\mathbf{x}} \rangle - \langle \mathbf{S}_{\mathbf{R}_i} \cdot \mathbf{S}_{\mathbf{R}_i+\mathbf{y}} \rangle$ and $\Phi_{B_{1g}} = \langle \mathbf{S}_{\mathbf{R}_i} \cdot \mathbf{S}_{\mathbf{R}_i+\mathbf{x}+\mathbf{y}} \rangle - \langle \mathbf{S}_{\mathbf{R}_i} \cdot \mathbf{S}_{\mathbf{R}_i-\mathbf{x}+\mathbf{y}} \rangle$.

It is also interesting to look at the related $CsFe_2As_2$ compound which shows a tendency towards B_{1g} nematicity as well, although long-range order seems absent.[13,15] In our simulations, the aforementioned magnetic configurations are unstable in $CsFe_2As_2$ for the parameter choice $s = 0.85$. Smaller fluctuations corresponding to $s = 0.90$ allow for stable double-stripe and Néel orders where the former is lower in energy, similarly to $RbFe_2As_2$. All this suggests that $CsFe_2As_2$ has a weaker tendency towards the B_{1g} nematicity than its Rb-counterpart, consistent with the experimental findings.

Finally, the experimental[18,26] and theoretical indications[20,22,42] that electronic correlations are stronger in hole-doped AFe_2As_2 iron pnictides as compared to $AeFe_2As_2$ could also be an aspect contributing to the change in the nature of nematicity in these systems. In the present work, we concentrated on the underlying magnetism and found strong hints of its role in determining the various nematic phases.

Conclusions. In summary, our first-principles calculations of the magnetic ground states of 122-type iron-based compounds show that the dominant magnetic instability in these systems is strongly affected by the nature of the spacer cation substitution. For $RbFe_2As_2$,

we found that the double-stripe state becomes the leading instability, in contrast to the single-stripe order in $SrFe_2As_2$. Analysis of the various contributions involved in the calculations showed that the magnetic order is more sensitive to the electron count variation due to the Sr→Rb substitution than to the related structural changes. Based on these results, we proposed that the evolution of the nematic state from B_{2g} for $SrFe_2As_2$ to B_{1g} for $RbFe_2As_2$ is a consequence of the change in the vestigial ordered states supported by the single-stripe and double-stripe orders.[48]

Our results have important experimental consequences that can in principle be verified. First, even though $RbFe_2As_2$ is not magnetic, it should have strong magnetic fluctuations peaked at the $\mathbf{Q}_3 = (\pi/2, \pi/2)$ wavevector, present above the nematic transition and enhanced below it. In contrast, the mechanism proposed in Ref. [16] relies on incommensurate fluctuations. To the best of our knowledge, there are no inelastic neutron scattering measurements available for $RbFe_2As_2$, which could distinguish between these two scenarios. Neutron scattering in the related $n_d = 5.5$ KFe_2As_2 compound reveals incommensurate spin fluctuations peaked at $(\pi(1\pm2\delta), 0)$ with $\delta \approx 0.16$,[43] which, according to our model, is consistent with the absence of B_{1g} nematic order in this system. Also, our phase diagram in Fig. 1 shows that uniaxial strain along the c-axis can tune the magnetic ground state for compounds with intermediate levels of hole doping. This offers the possibility to tune the nematic state from B_{2g} to B_{1g} as a function of strain or pressure.

Acknowledgments

We thank T. Shibauchi and J. Schmalian for fruitful discussions. VB and RV were financially supported by DFG Sonderforschungsbereich TRR 49. The computer time was allotted by the centre for supercomputing (CSC) in Frankfurt and by the computer center of Goethe University. RMF was supported by the U.S. Department of Energy, Office of Science, Basic Energy Sciences under award number DE-SC0012336. Parts of some figures have been produced with VESTA3 (Ref. 44).

* Corresponding author: borisov@itp.uni-frankfurt.de

[1] P. J. Hirschfeld, M. M. Korshunov, and I. I. Mazin, Reports on Progress in Physics **74**, 124508 (2011).
[2] A. Chubukov, Annual Review of Condensed Matter Physics **3**, 57 (2012).
[3] D. C. Johnston, Advances in Physics **59**, 803 (2010).
[4] P. C. Canfield and S. L. Bud'ko, Annual Review of Condensed Matter Physics **1**, 27 (2010).
[5] H.-H. Wen and S. Li, Annual Review of Condensed Matter Physics **2**, 121 (2011).
[6] R. M. Fernandes, A. V. Chubukov, and J. Schmalian, Nature Physics **10**, 97 (2014).
[7] R. M. Fernandes, A. E. Böhmer, C. Meingast, and J. Schmalian, Phys. Rev. Lett. **111**, 137001 (2013).
[8] A. E. Böhmer and C. Meingast, Comptes Rendus Physique **17**, 90 (2016), iron-based superconductors / Supraconducteurs a base de fer.
[9] C. Xu, M. Müller, and S. Sachdev, Phys. Rev. B **78**, 020501(R) (2008).
[10] C. Fang, H. Yao, W.-F. Tsai, J. P. Hu, and S. A. Kivelson, Phys. Rev. B **77**, 224509 (2008).
[11] R. M. Fernandes, A. V. Chubukov, J. Knolle, I. Eremin, and J. Schmalian, Phys. Rev. B **85**, 024534 (2012).
[12] S. Liang, A. Moreo, and E. Dagotto, Phys. Rev. Lett. **111**, 047004 (2013).
[13] J. Li, D. Zhao, Y. P. Wu, S. J. Li, D. W. Song, L. X. Zheng, N. Z. Wang, X. G. Luo, Z. Sun, T. Wu, and X. H. Chen, arXiv:1611.04694 (2016).
[14] X. Liu, R. Tao, M. Ren, W. Chen, Q. Yao, T. Wolf, Y. Yan, T. Zhang, and D. Feng, Nat. Commun. **10**, 1039 (2019).
[15] K. Ishida, M. Tsujii, S. Hosoi, Y. Mizukami, S. Ishida, A. Iyo, H. Eisaki, T. Wolf, K. Grube, H. v. Löhneysen, R. M. Fernandes, and T. Shibauchi, arXiv:1812.05267 (2018).
[16] S. Onari and H. Kontani, Phys. Rev. B (Rapid Communication) **100**, 020507 (2019).
[17] C.-Y. Moon and H. J. Choi, Phys. Rev. Lett. **104**, 057003 (2010).
[18] F. Hardy, A. E. Böhmer, L. de' Medici, M. Capone, G. Giovannetti, R. Eder, L. Wang, M. He, T. Wolf, P. Schweiss, R. Heid, A. Herbig, P. Adelmann, R. A. Fisher, and C. Meingast, Phys. Rev. B **94**, 205113 (2016).
[19] Z. P. Yin, K. Haule, and G. Kotliar, Nature Materials **10**, 932 (2011).
[20] L. de' Medici, G. Giovannetti, and M. Capone, Phys. Rev. Lett. **112**, 177001 (2014).
[21] J. Diehl, S. Backes, D. Guterding, H. O. Jeschke, and R. Valentí, Phys. Rev. B **90**, 085110 (2014).
[22] S. Backes, H. O. Jeschke, and R. Valentí, Phys. Rev. B **92**, 195128 (2015).
[23] L. Ortenzi, I. I. Mazin, P. Blaha, and L. Boeri, Phys. Rev. B **86**, 064437 (2012).
[24] L. Ortenzi, H. Gretarsson, S. Kasahara, Y. Matsuda, T. Shibauchi, K. D. Finkelstein, W. Wu, S. R. Julian, Y.-J. Kim, I. I. Mazin, and L. Boeri, Phys. Rev. Lett. **114**, 047001 (2015).
[25] M. Tegel, M. Rotter, V. Weiß, F. M. Schappacher, R. Pöttgen, and D. Johrendt, Journal of Physics: Condensed Matter **20**, 452201 (2008).
[26] F. Eilers, K. Grube, D. A. Zocco, T. Wolf, M. Merz, P. Schweiss, R. Heid, R. Eder, R. Yu, J.-X. Zhu, Q. Si, T. Shibauchi, and H. v. Löhneysen, Phys. Rev. Lett. **116**, 237003 (2016).
[27] G. Kresse, and J. Hafner, Phys. Rev. B (Rapid Communications) **47**, 558 (1993).
[28] N. Colonna, G. Profeta, A. Continenza and S. Massidda, Phys. Rev. B **83**, 094529 (2011).
[29] M. Tomić, R. Valentí, and H. O. Jeschke, Phys. Rev. B **85**,

094105 (2012).
[30] ELK FP-LAPW code (http://elk.sourceforge.net/).
[31] J. P. Perdew, K. Burke, and M. Ernzerhof, Phys. Rev. Lett. **77**, 3865 (1996).
[32] R. J. McQueeney, S. O. Diallo, V. P. Antropov, G. D. Samolyuk, C. Broholm, N. Ni, S. Nandi, M. Yethiraj, J. L. Zarestky, J. J. Pulikkotil, A. Kreyssig, M. D. Lumsden, B. N. Harmon, P. C. Canfield, and A. I. Goldman, Phys. Rev. Lett. **101**, 227205 (2008).
[33] Q. Huang, Y. Qiu, W. Bao, M. A. Green, J. W. Lynn, Y. C. Gasparovic, T. Wu, G. Wu, and X. H. Chen, Phys. Rev. Lett. **101**, 257003 (2008).
[34] C. de la Cruz, Q. Huang, J. Lynn, J. Li, W. Ratcliff II, J. Zarestky, H. Mook, G. Chen, J. Luo, N. Wang, and P. Dai, Nature **453**, 899 (2008).
[35] I. Opahle, H. C. Kandpal, Y. Zhang, C. Gros, and R. Valentí, Phys. Rev. B **79**, 024509 (2009).
[36] R. M. Fernandes, P. P. Orth, and J. Schmalian, Annual Review of Condensed Matter Physics **10**, 133 (2019).
[37] I. Paul, A. Cano, and K. Sengupta, Phys. Rev. B **83**, 115109 (2011).
[38] G. Zhang, J. K. Glasbrenner, R. Flint, I. I. Mazin, and R. M. Fernandes, Phys. Rev. B **95**, 174402 (2017).
[39] C. B. Bishop, J. Herbrych, E. Dagotto, and A. Moreo, Phys. Rev. B **96**, 035144 (2017).
[40] J. J. Wu, J. F. Lin, X. C. Wang, Q. Q. Liu, J. L. Zhu, Y. M. Xiao, P. Chow, and C. Q. Jin, Scientific Reports **4**, 3685 (2014).
[41] J. K. Glasbrenner, I. I. Mazin, H. O. Jeschke, P. J. Hirschfeld, R. M. Fernandes, and R. Valentí, Nature Physics **11**, 953 (2015).
[42] F. Hardy, A. E. Böhmer, D. Aoki, P. Burger, T. Wolf, P. Schweiss, R. Heid, P. Adelmann, Y. X. Yao, G. Kotliar, J. Schmalian, and C. Meingast, Phys. Rev. Lett. **111**, 027002 (2013).
[43] C. H. Lee, K. Kihou, H. Kawano-Furukawa, T. Saito, A. Iyo, H. Eisaki, H. Fukazawa, Y. Kohori, K. Suzuki, H. Usui, K. Kuroki, and K. Yamada, Phys. Rev. Lett. **106**, 067003 (2011).
[44] K. Momma and F. Izumi, J. Appl. Cryst. **44**, 1272 (2011).
[45] Y. Wang, W. Hu, R. Yu, and Q. Si, arXiv:1903.00375 (2019).
[46] The sufficient accuracy of the chosen DFT approach is indicated by the fact that, when optimized, the structures of the end compounds would agree well with the measured ones (more details in Section 2 of the SI, which includes Refs. [27–29]). Throughout the manuscript, however, the room-temperature experimental structures were used.
[47] We note that, in our simulations, the single-stripe order remains the ground state of $SrFe_2As_2$ even for smaller values of s, as illustrated by Fig. S1 in the SI.
[48] Recently a different scenario of nematicity has been proposed.[45]